

Sensor payloads for small unmanned aerial vehicles

Rusty Trainham,^{1,a} Paul Guss,^b Manuel Manard,^a Lance McLean,^c Willy Kaye,^d Kevin Kochersberger^e

^a Special Technologies Laboratory, 5520 Ekwill St, Santa Barbara, CA 93111, USA

^b Remote Sensing Laboratory – Nellis, P.O. Box 98521, M/S RSL-09, Las Vegas, NV 89193-8521, USA

^c Remote Sensing Laboratory – Andrews, Building 1783, Arnold Avenue, Andrews AFB, MD 20762, USA

^d H3D Inc, 4692 Erin Ct, Ann Arbor, MI 48105, USA

^e Virginia Tech Univ, 119 Randolph Hall, 460 Old Turner St, Blacksburg, VA 24060, USA

ABSTRACT

Small unmanned aerial systems (sUAS) are ideal for delivering sensors into areas that are inaccessible or too dangerous for human entry or manned aircraft over-flights. The systems can fly low and slow for enhanced sensitivity, and they can get into tight spaces where ordinary aircraft would never attempt to fly. We have configured and flown sensor payloads for radiation, chemical, and optical detection on small fixed wing and rotary wing aircraft. For radiation detection we have flown packages consisting of sodium iodide (NaI), lanthanum bromide (LaBr₃), and cadmium-zinc-telluride (CZT) gamma spectrometers, and we have also flown a CZT gamma imaging detector. The chemical sensing package consists of surface catalytic detectors for real-time chemical sensing, and a multi-tube chemical sampler that can be post-flight analyzed with a gas chromatograph mass spectrometer (GCMS). The optical package comprises a small spectrometer with wavelength sensitivity from 200 nm to 900 nm, and it has successfully collected burst light spectra from small explosive detonations. All the sensor packages provide telemetry, GPS coordinates, LIDAR distance ranging, and absolute time of day to microsecond accuracy. Payload weights range from less than 1 kg up to 5.5 kg, and they have flown on Sandstorm and T-28 fixed wing drones, on a custom-built heavy-lift hex-copter, a 3DR Solo quad-copter, and a T-Rex 700 helicopter. Communications are over 2.4 GHz, 915 MHz radios, and 4G LTE cellular data links. Real time data feeds from the sensor payloads to web browser clients anywhere in the world are possible via a virtual server on the Amazon AWS cloud.

Keywords: unmanned aerial systems, radiation detection, chemical detection, optical spectroscopy

Introduction

Detectors for radiation, chemical, and spectroscopic real time sensing have been developed for fixed wing and rotary unmanned aerial vehicles. The systems have been flight tested in Idaho, Montana, Nevada, and Wisconsin, and have demonstrated radiation detection from an aerial asset, mapping of radioactive contamination, real time chemical sensing, chemical sampling for post-flight analysis, and the capture of optical spectra from small detonations. Although bench top testing of the systems is essential during

¹ trainhpc@nv.doe.gov, 805-681-2248

UNCLASSIFIED

development, it is not a replacement for actual fight testing. Operating detectors on aerial platforms is challenging, and we experienced a few mishaps while testing in difficult environments.

Mapping and characterizing radioactive contamination after a nuclear or radiological accident is a hazardous operation for which drones are ideally suited. In the aftermath of the Fukushima nuclear meltdown radiation levels in the vicinity of the reactors were lethal, so personnel were unable to make measurements in critical locations. Even aerial surveys had to avoid direct low altitude overflights of the reactor containment structures to limit personnel exposure. Replicating such an environment for testing drone borne detector operations is challenging, because of real risks to personnel and equipment of radioactive contamination during the tests. Another scenario for radiation detection is searching, locating, and characterizing a radioactive source. Tests of this scenario are considerably easier, since the radiation hazards are easily contained and managed.

Factory accidents and refinery fires are compelling use cases for drone borne chemical detection. Smoke sampling for the situational awareness of firefighters is another, and characterizing the chemical composition and lethality of releases from improvised chemical explosive devices (ICED) is yet another. The obvious first tests in developing drone borne chemical detecting capabilities are single point sampling for small but lethal releases, and plume mapping over large extended contamination areas. The questions to be answered are “What is it?”, “Where is it?”, and “How far does it extend?” We have developed two detector systems. One for the fixed-wing Sandstorm, and one for the 3DR Solo quadcopter. They both use the same technologies, but were scaled for the different platforms. The Sandstorm version is a seven-pound detector, and the 3DR Solo version weighs less than two pounds.

Positioning an optical spectrometer close to a detonation or a flame by a drone is another scenario that we have tested. This can be useful for situations which do not allow for direct line of sight with a telescope based spectrometer. The spectrometer is small enough that a drone can also carry a chemical detector along with it to provide more information. This combination could be useful for assessing conditions of back country wild fires or of chemical or petroleum facility fires.

Flying detectors on drones is not without risk, and mishaps can occur suddenly and unexpectedly. This year we lost an hex-copter during a test flight in Idaho. Fortunately, the expensive detector it was carrying survived the crash. Other incidents occurred that could have been serious, but were not, either because we caught and corrected problems in time, or simply because we were lucky. Test conditions in the places where we fly can be severe, and replicating the density altitude, temperature, humidity, wind, and dust conditions in the laboratory or at a training field is not always feasible. Our test venues can be brutal places to fly, which makes them particularly valuable, because success in those venues is an ultimate test of survivability. From the Idaho crash we learned that the Sandstorm pod, which consists of a suspended tray within a reinforced fiberglass shell, offers robust protection of the instrumentation within. We also learned that the Raspberry Pi is an excellent single board computing solution for detector operations on a drone. It runs for hours on a small battery, has adequate computing power for our detectors, and is mechanically very robust. It survived two severe crashes and booted again after the sand was blown out.

A few of the platforms that we have flown do not provide any infrastructure for detector operations, so we improvised a solution with a Raspberry Pi 3B powered by a battery. The Raspberry Pi is single board computer about the size of a credit card, and it is housed in a box somewhat thicker than a deck of playing cards. Inside of the box with the Raspberry Pi is an Adafruit Ultimate GPS receiver, and attached to the outside of the box is an Adafruit 10 DOF (10 degrees-of-freedom) card for flight telemetry (accelerations, rotations, altitude, and compass heading). The GPS receiver conveniently provides a one pulse per second (1PPS) strobe that we have routed to the GPIO header of the Raspberry Pi. This is used to lock the Raspberry Pi’s system clock to GPS time, and it is accurate to within several tens of microseconds of

UNCLASSIFIED

UNCLASSIFIED

absolute time of day. Fiducial time stamps in the data streams from the system clock are used to correlate sensor data to GPS location and flight telemetry.

The 10DOF provides telemetry data (accelerometer, magnetometer, gyro, barometric pressure, and temperature), and the card communicates over the I2C bus to the Raspberry Pi, providing data five times per second. The barometer and temperature readings are used to calculate pressure altitude in real time by a C program running on the Raspberry Pi.

Altitude above ground is measured by a Lightware SF11/C single point LIDAR range finder. For Sandstorm operations it is plugged into one of the USB ports of the Raspberry Pi, and it is monitored by a program written in C. For the 3DR Solo it shares the same USB connection as the detector, and it is monitored by a program written in Python. In both cases LIDAR readings are merged with the 10DOF data and written to the same log file. The LIDAR reading is also separately mirrored by a memory mapped file for real time access.

Several options exist for communications to the ground station. The Raspberry Pi 3B has on-board ethernet, wifi, bluetooth, USB, and serial ports. For short range communications wifi is very convenient, and is a commonly used link when the aircraft is on the ground. For longer range service a 915 MHz radio is normally the aerial communications link. If the test venue has a nearby cell tower providing 4G cellular service, then a cell phone data link becomes an option. However, most of our test flights have occurred in areas with poor cellular reception. Finally, we have also used ethernet interface to connect to 2.4 GHz Ubiquiti Unifi hardware, providing communications over a single radio link for both aircraft and sensor payload.

Real time access to the pod's data stream over the Internet is possible by means of a virtual server on the Amazon EEC cloud. The server transparently redirects external client connections through an ssh tunnel to the pod's Raspberry Pi. The client computer requires no special software nor any configuration changes, and simply directing a web browser to the IP number of the virtual server is sufficient to stream data from the Raspberry Pi. This means that the pod itself must have Internet access, either through the ground station, or over a cellular link directly from within the pod. The limited bandwidth of the pod's radio link does not make this solution scalable if numerous clients desire access. A better solution would be for the server to mirror the pod's data in real time and handle external clients without redirection.

Aircraft

The Sandstorm is a fixed wing drone with a 15 foot wingspan made by Unmanned Systems Incorporated. It is powered by a pusher turbo prop, and it can carry up to 20 pounds of payload for two hours. The autopilot on-board is a Piccolo Nano, and it communicates to the ground over 915 MHz and 2.4 GHz radio links. The Sandstorm does not provide power, communications, GPS, or telemetry to a sensor payload, so it is essentially an aerial test bench. This lack of infrastructure imposes added complexity to the design of a sensor payload, but it also simplifies the engineering of installing a sensor on the Sandstorm. Self-contained payloads are quickly installed and removed, and the turn-around time for payload interchange is about 15 minutes. Figure 1 shows the Sandstorm with the chemical detector in the belly pod. The Sandstorm has carried five different radiation detector payloads in various test flights.

Figure 1 also shows a 3DR Solo quadcopter with a 2x2 NaI radiation detector strapped to its expansion bay. The Solo can lift a 1 kg payload for a flight time of about 10 minutes. On the Solo we have flown two types of radiation detectors (NaI & CZT), a chemical detector, and an optical spectrometer. The expansion port on the chassis bottom provides access to raw battery power, regulated 5 volts, and the USB interface to the Solo's on-board iMX6 computer. The operating system is Yocto Linux. There are no development libraries included in the 3DR Solo as distributed by 3DR, but the necessary libraries can be

UNCLASSIFIED

UNCLASSIFIED

installed from the Yocto Linux repositories. A C compiler and the USB development library are required to build the code to operate the gamma detector.



Figure 1. Left: The USI Sandstorm with the chemical detector during an exercise in Montana. Right: The 3DR Solo has a 2x2 NaI(Tl) radiation detector strapped to the expansion bay.

The left side photo of Fig. 2 shows the Virginia Tech heavy lift hex-copter carrying the Apollo and 2x2 NaI detectors for a combined payload weight of 13 pounds. The photo was taken during an exercise at the Radiological Response Training Range (RRTR) of Idaho National Laboratory (INL). The right side photo of Fig. 2 shows the Apollo detector mounted on a T-Rex 700 RC helicopter. The payload weight of this configuration is 7 pounds.



Figure 2. Left: The Virginia Tech hex-copter is carrying the Apollo detector and a 2x2 NaI(Tl) detector during an exercise at INL's RRTR. Right: The Apollo detector is strapped to a T-Rex 700 RC helicopter.

Radiation Detection

Radiation detection represents the bulk of our efforts to date in equipping drones with sensors. We have flown several NaI detectors with sizes ranging from 1x1 up through 3x6 on all of the flight platforms. We have also flown Cadmium Zinc Telluride (CZT) and Lanthanum Bromide (LaBr_3) detectors, as well as a Geiger counter. Of particular interest is the Apollo detector developed by H3D Corporation of Ann Arbor, Michigan.

UNCLASSIFIED

UNCLASSIFIED

Apollo Detector

The Apollo detector is a hand held gamma imager commercially available from H3D. It has four 20mm x 20mm x 15mm CZT crystals mounted on a segmented anode and backed by a Peltier cooler. The anode is an 11 x 11 grid, providing x - y positional sensing of a gamma interaction within the CZT crystal. The z coordinate of the interaction is derived from the difference in drift times of charge carriers to the anode vs cathode. The data consist of gamma energy, x - y - z location, a time stamp, and the number of correlated interactions occurring within a defined time window. The correlations are primarily due to Compton scattering, and the locations of the correlated interactions define a vector for back-projecting to a probable origin of the gamma. Statistically, the back-projections can be used to construct a gamma image of the radioactive source.

The version of Apollo that we tested had its form factor re-engineered by H3D to fit within the Sandstorm pod. It is a self-contained unit with its own battery, but it does not have on-board GPS or telemetry. Access to the Apollo is through H3D's on-board graphical interface. Although the graphical interface is accessible over wifi, ethernet, and cellular data links, its bandwidth requirement is too much for the 915 MHz radio link. Since the 915 MHz radio is the most common communications link to the pod, some accommodations had to be made. The Raspberry Pi was already needed in the pod to provide GPS and telemetry, so it was configured to access the Apollo and pull a subset of real time data and make it available over the low bandwidth 915 MHz link. Average spectra and region of interest (ROI) gamma intensity readings are accessible in real time through the Raspberry Pi's web server, and starting and stopping Apollo data acquisitions are triggered via the Raspberry Pi's web server. Figure 3 shows the Apollo pod mounted on the Virginia Tech hex-copter.

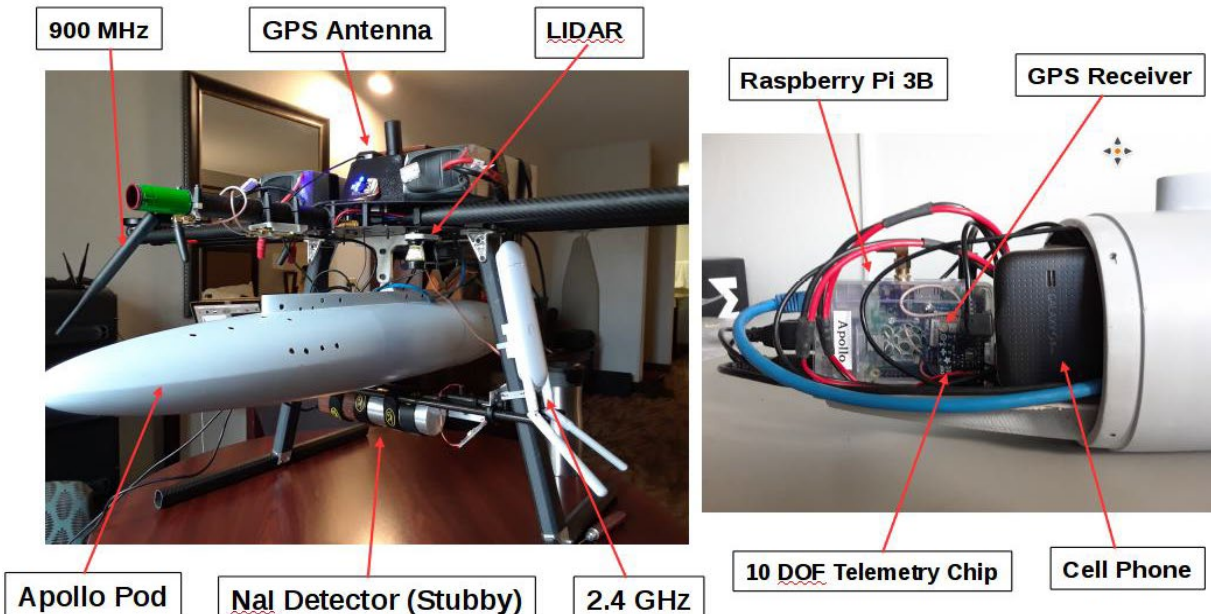


Figure 3. Photos of the Apollo pod on the Virginia Tech hex-copter are labeled to show various components. The right photo is a close-up of the pod with the nose cone removed.

Figure 4 shows some results from a radiation mapping exercise at the RRTR in Idaho. Radioactive bromine (^{82}Br) was explosively dispersed in three craters at the training range for an emergency response exercise. This isotope was chosen because of its short 35.3 hour half-life, so that any contaminated instrumentation would be clean again within two weeks' time, as the radioactive bromine decayed into stable krypton. The plot on the left of Fig. 4 is the gamma

UNCLASSIFIED

UNCLASSIFIED

spectrum of ^{82}Br measured by the Apollo detector, and the satellite photo on the right shows the flight path over one of the craters weighted by the radiation signal mapping the contamination area.

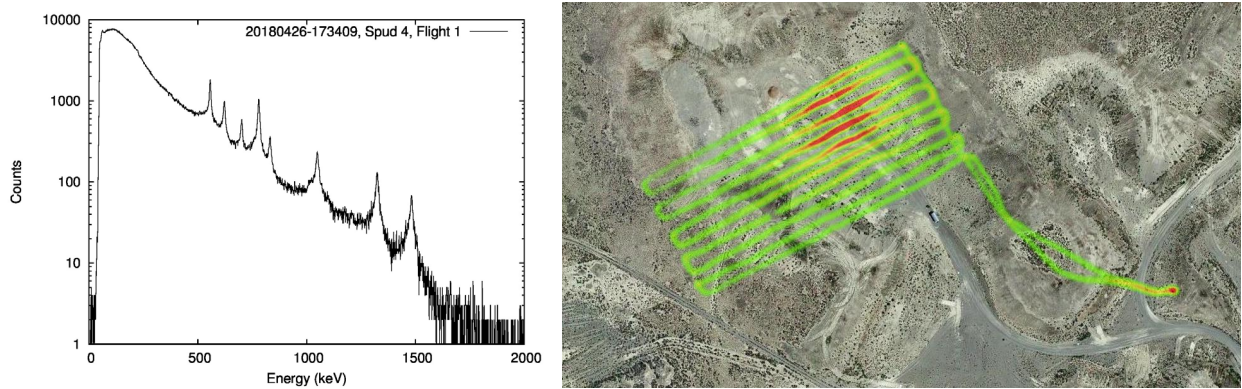
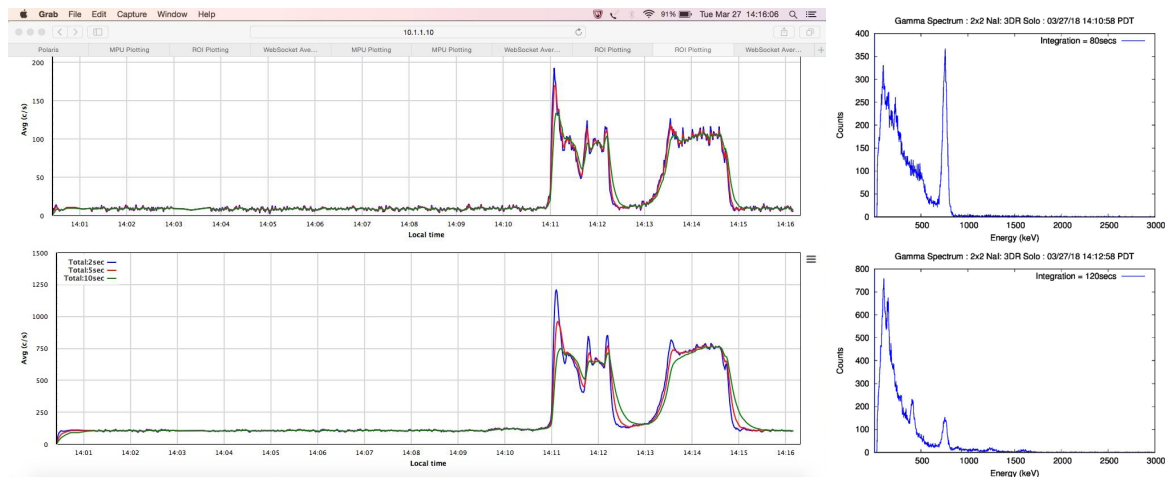


Figure 4. The gamma spectrum measured by the Apollo detector in flight is clearly from ^{82}Br , and the aerial photo shows the geographic distribution of radioactive contamination at the RRTR in Idaho.

Quadcopter borne 2x2 NaI detector

A 2x2 NaI(Tl) gamma detector is at the weight limit for payload on a 3DR Solo. Initial flights with an off the shelf 2x2 NaI(Tl) detector were successful, but the flight stability was marginal due to the low center of gravity and large moment arm of the detector. Consequently, we asked Alpha Spectra to manufacture a modified “stubby” version of the detector which is 2 inches shorter and 4 ounces lighter than the standard detector. Referring back to Fig. 1 the modified “stubby” NaI detector is shown strapped to the bottom of the 3DR Solo. This configuration has better flight stability, and the performance of the detector is comparable to that of a standard detector.

Figure 5 shows results from a test of the stubby NaI on the Solo flying over two radioactive sources. The graph on the left is a screen capture of the web page showing the radiation signal as a function of time. The two plots on the right are spectra generated from the list mode data while hovering over each source. The first source was ^{137}Cs , and the second was ^{152}Eu . The ^{152}Eu spectrum also shows signal from ^{137}Cs . The sources were 50 meters apart, and the Solo hovered at an altitude of 25 meters. The ^{137}Cs source was a much stronger source, and the ^{152}Eu was not placed far enough away to completely separate the radiation signals.



UNCLASSIFIED

UNCLASSIFIED

Figure 5. On the left is a screen capture of the radiation signal collected by the 3DR Solo as it flew over two radioactive sources. The spectra on the right are data collected while over each source. The upper is ^{137}Cs , and the lower is ^{152}Eu with some ^{137}Cs bleed-over.

Sandstorm borne chemical detection

The chemical detector for the Sandstorm consists of a volatile organic compound (VOC) sensor chip and a vacuum sampler. Referring back to Fig. 1 the chemical sampler is in the pod mounted beneath the Sandstorm, and the VOC chip can be seen on a rod extending forward of the wing. The vacuum sampler comprises six tubes of Carbotrap 300 adsorbent to capture volatile organics for post flight analysis. The sampler does not provide data in real time, however the VOC chip does provide real time data. The VOC chip is an Amphenol SGX Sensortech MiCS-5524 powered by 5 volts, and it outputs an analog voltage. A Texas Instruments ADS1015 analog to digital converter (ADC) measures the output of the VOC chip and communicates it over the I2C bus to the Raspberry Pi.

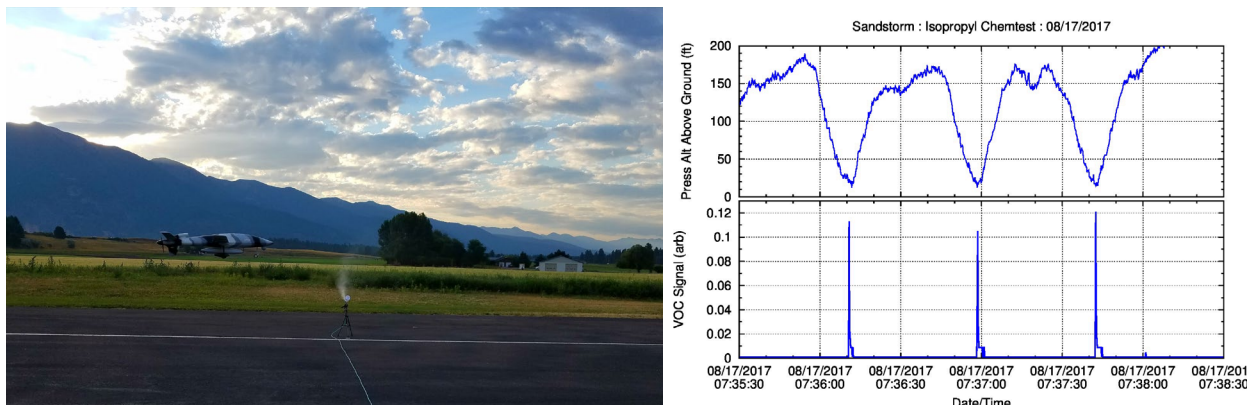


Figure 6. The Sandstorm is about to fly through a small alcohol plume from a sprayer on the runway at the USI airfield in Kalispell, Montana. The plots on the right show the pressure altitude (upper) and voltage from the VOC chip (lower). The time within the plume was a fraction of a second.

The original idea for the first chemical test was to use an RC helicopter to lift a liter of a common solvent, such as alcohol or acetone to an altitude of 100 feet and rapidly release it within the flight path of the Sandstorm. The logistics of coordinating the two flights and performing the chemical release were not difficult, however, the plume dynamics in any wind condition other than complete calm were prohibitive. Several seconds would be required to assure that the helicopter was out of the way of the Sandstorm, during which time the chemical dispersed too rapidly to be detectable once the Sandstorm reached the site of the plume. The minimum speed of the Sandstorm, being 40 knots, meant that its time within the plume would be only a fraction of a second. A fallback option was to build a bonfire at the end of the runway, however the schedule for the test slipped from the spring into late summer, which was fire season in Montana. We settled upon placing a sprayer on the runway and flying the Sandstorm at very low altitude through the sprayer's small plume.

The Sandstorm is not an ideal platform for chemical sensing, because it flies through a plume too quickly, and during the test in Montana it was only a fraction of a second. The sampler's small pump can only move 100 ml/min through a sample tube, so the detection sensitivity is severely limited. A rotary platform would be more appropriate, since it can hover for arbitrary durations for adequate air sampling. After the Montana test we decided to develop a chemical detector for the 3DR Solo quadcopter.

UNCLASSIFIED

UNCLASSIFIED

Quadcopter borne chemical detection

The concept of the quadcopter chemical detector is identical to that of the Sandstorm, but downsized to fit the small 3DR Solo. The new sampler consists of a vacuum pump and a single Carbotrap 300 sample tube. However, it includes a second VOC sensor chip to supplement the MiCS-5524. We chose an MQ-135 as the second sensor because it detects smoke, ammonia, benzene, as well as some nitrogen and sulfur compounds.

The I2C bus on the 3DR Solo is not accessible from its expansion port, so rather than performing surgery on the Solo to connect to the I2C bus we opted to use the Solo's USB interface. This required an intermediate circuit to provide digital I/O and ADC readings, and for this we utilized a Teensy 3.2, which is an Arduino-style micro-controller. The code to control the Teensy is written in a C-like language and was developed in the Arduino integrated development environment (IDE).

The test of the Solo's chemical detector was flown over four garbage cans of kerosene and acetone soaked burning rags. To avoid unnecessary fire hazards we chose to conduct the test during a rainy week in Antigo, Wisconsin. The Solo flew on autopilot over a grid pattern while collecting smoke and measuring real time signals from the VOC chips. The smoke sample was then analyzed post-flight with a gas chromatograph mass spectrometer (GC Mass Spec).

The left photo in Fig. 7 shows the 3DR Solo in flight over the fires, and the right photo shows the 3DR controller with the flight plan displayed on the attached tablet computer. The flight plan was composed in an Android version of Mission Planner called Tower, and the plan uploaded from the tablet to the quadcopter over the 3DR controller's wifi.



Figure 7. The 3DR Solo is flying with the chemical sensor over four garbage cans of kerosene and acetone soaked burning rags in Antigo, Wisconsin. The tablet computer attached to the 3DR controller displays the flight plan that was uploaded to the quadcopter.

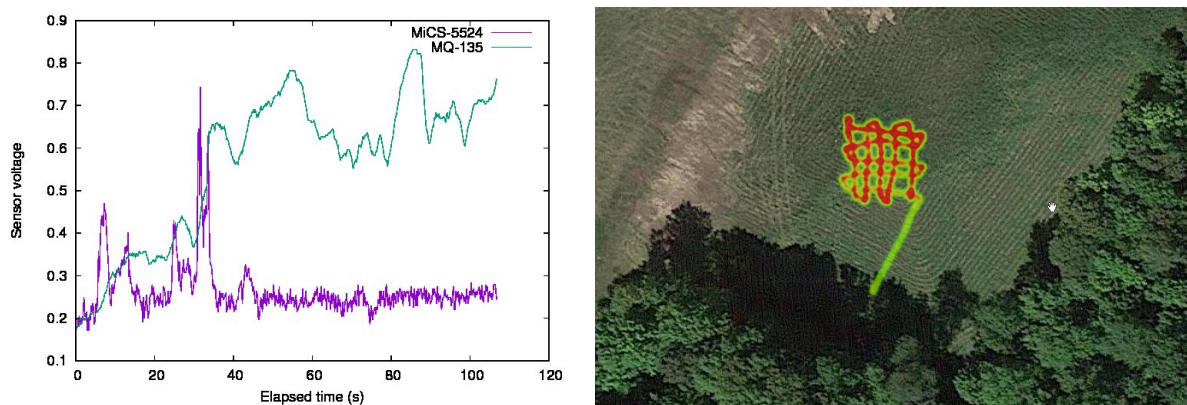
As we discovered during the previous chemical test with the Sandstorm, simulating the plume conditions of a chemical disaster can be difficult. Although the fires in Wisconsin generated a much larger plume than the sprayer, the plume was still very susceptible to winds. During the initial test flight with the Solo we discovered that prop wash can have a profound effect on the plume. For successive flights we

UNCLASSIFIED

UNCLASSIFIED

mounted the VOC chips and the vacuum collection tube on a carbon fiber rod to extend them outside of the prop wash. This solution was not ideal since it merely delayed the onset of the prop wash effect rather than eliminate it.

The reason for flying two VOC chips was to test the MQ-135, having the MiCS-5524 as a control. The MQ-135 provides sensitivity to sulfur compounds, and we had originally intended to add a sulfur based herbicide to the flames for later flights. However, we discovered on the initial flight that the MQ-135 chip's response and recovery to smoke exposure was very slow. The plot on the left of Fig. 8 shows the response of the two VOC chips while flying over the fires, and the satellite photo on the right displays the GPS tracks weighted by the MQ-135 signal. In light of the problematic response of the MQ-135, and of the inconvenience of having the plume disrupted by the prop wash, we decided to scrap the idea of burning any sulfur compounds for the remaining flights of the test.



Filter 8. Real time signals from the VOC chips show that the MQ-135 chip was slow to respond and recover from smoke exposure. The satellite photo shows the flight path weighted by the MQ-135 signal. Because of the slow response no plume distribution mapping is possible from the data.

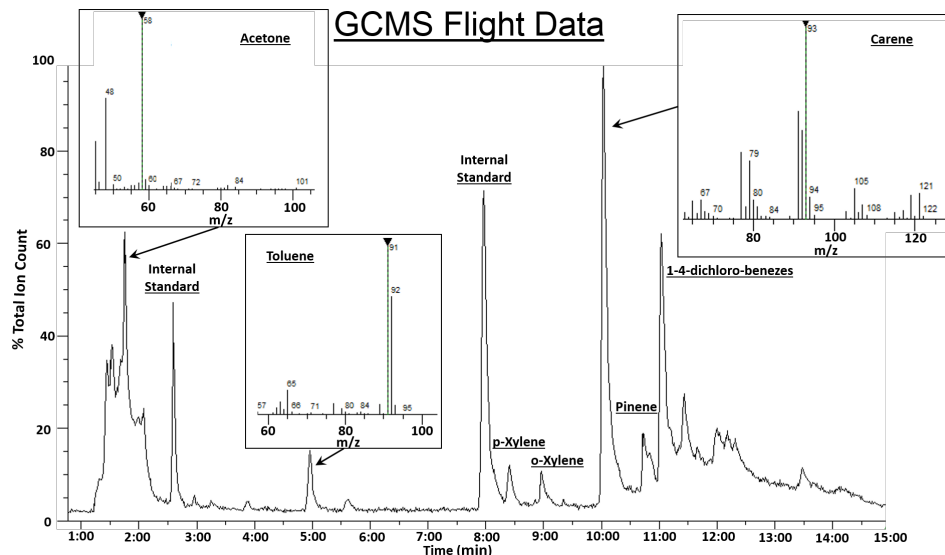


Figure 9. Post flight analysis of the sample collected by the Carbotrap 300 show toluene from the kerosene, as well as unburned acetone. The peaks of carene and pinene are from combustion products from burning polyester rags.

UNCLASSIFIED

UNCLASSIFIED

Figure 9 shows results from the GC mass spectrometer of the smoke collected by the vacuum sampler. The toluene peak indicates the presence of unburned kerosene. The acetone peak is present because we burned both acetone and kerosene for that test flight. Several compounds (carene, pinene, etc.) are combustion products from burning polyester. Some of the rags were polyester clothing purchased at a thrift store.

Optical Spectroscopy

The chemical test in Wisconsin also provided an opportunity to fly an optical spectrometer on the 3DR Solo. The spectrometer is an Ocean Optics Flame-S, which is sensitive from 200 nm to 900 nm. The computer code to run it on the 3DR Solo was ported with minimal changes from a previous version developed for the Raspberry Pi. The photo on the left of Fig. 10 shows the Solo in flight carrying the spectrometer. The photo on the right is a close-up of the Solo with the spectrometer, a GoPro camera, a Lightware SF-11/C LIDAR, a Teensy 3.2, and two VOC sensor chips. The laptop computer in the photo displays a spectrum of an LED flash light used to align the fiber telescope on the Solo. That spectrum is being displayed in real time by an html page served from a web server on the Solo.



Figure 10. On the left the 3DR Solo is shown in flight carrying the Ocean Optics spectrometer. The photo on the right shows the Solo with spectrometer, a GoPro camera, and two VOC sensor chips. The laptop is displaying a real time spectrum of an LED flashlight used to align the optics.

To test the drone borne spectrometer we sought out a scenario similar previous spectroscopic work we have done with explosives at BEEF [BEE13]. We accomplished this by collecting data from a series of small detonations of Tannerite. This chemical is reputed to be a mixture of aluminum powder with ammonium nitrate and ammonium perchlorate. We expected to see strong bands of aluminum oxide emissions, but the spectra shown in Fig. 11 show no evidence of aluminum combustion. The spectra do, however, show emissions from sodium and potassium, which are commonly seen in dirty combustion, and, surprisingly, a strong unexpected emission from lithium at 671 nm.

UNCLASSIFIED

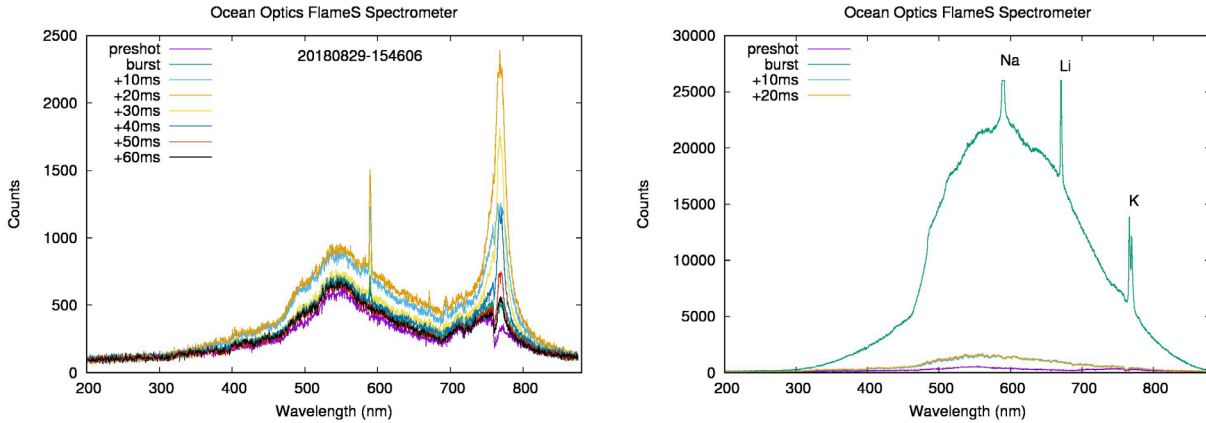
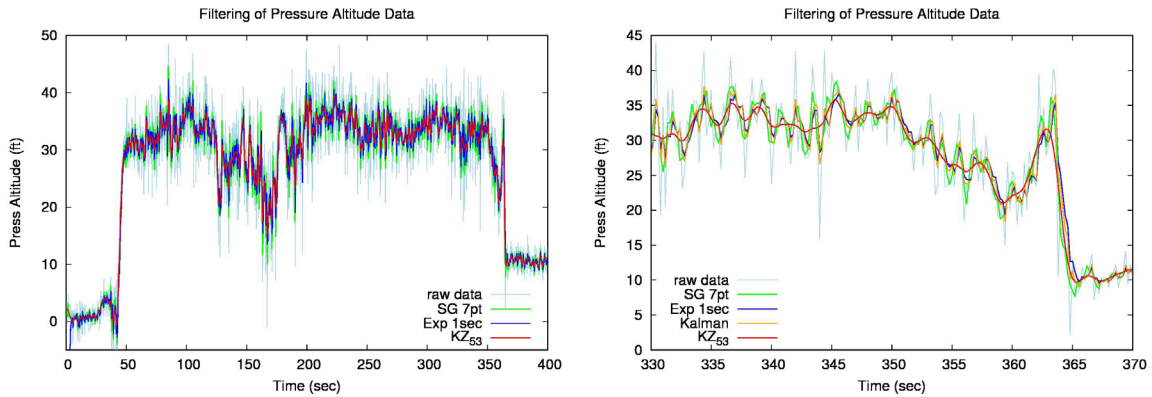


Figure 11. Spectra from a small Tannerite detonation collected by an Ocean Optics Flame-S spectrometer on a 3DR Solo show usual combustion contaminants of sodium and potassium, but do not show evidence of aluminum combustion. The lithium emission at 671 nm is unexpected.

Data Filtering

Data collected in flight tend to be noisy. Vibrations, rotations, temperature fluctuations, electromagnetic interference from motors, etc. are significant noise sources. With the copters another source of noise is barometer air buffeting by the prop wash. The barometer provides pressure altitude data, and Fig. 12 shows altitude data plotted with results from several algorithms filtering the noise. The plot on the left is of data from the full flight, and the plot on the right is a close-up of filter results at the end of the flight. The results shown are from Savitzky-Golay [SAV64], Kolmogorov-Zurbenko [YAN10], Kalman [KAL60], and exponential moving average [SMI97] filter routines. These filters can operate in real time on the Raspberry Pi, and during flights we normally use an exponential moving average, because it is a simple and effective filter. It does, however, introduce a phase lag, so we tested the other algorithms for suitability. In this example the smoothest curve is produced by the Kolmogorov-Zurbenko filter, but the curve has lost some real features in the data. This is a multiple order moving average filter that is complicated to implement and is more CPU intensive than the other filters. The Savitzky-Golay is a simple moving polynomial fit whose order that can be chosen at will. It is fairly simple to implement, and it has minimal artifacts. The Kalman filter is also rather simple to implement, and it produces reasonable results. All of these filters have tunable parameters, so the results shown here are not necessarily optimal. There is no clear winner.



UNCLASSIFIED

UNCLASSIFIED

Figure 12. Raw pressure altitude data are plotted with results from several filter algorithms. SG 7 is a 7 point Savitzky-Golay filter, Exp 1 is an exponential moving average with a 1 second time constant, KZ53 is a 5 point triple pass Kolmogorov-Zurbenko filter, and Kalman is a linear Kalman filter.

Conclusion

We have developed and flight tested a variety of detectors for aerial measurements on fixed wing and rotary drones. Radiation detection is the most advanced of our capabilities to date. Currently we are only sensitive to gamma radiation, but soon we plan to test a CLYC detector which has neutron capability. Chemical detection is currently limited to volatile organic compounds, but we would like to extend the capability to include sulfur and phosphorus compounds. The spectroscopic sensitivity extends from 200 nm in the near ultraviolet through the visible to 900 nm in the near infrared. In the ultraviolet this extent is as far as it reasonably can be for any atmospheric application. Extending sensitivity further into the infrared would be desirable, because adding a hyper-spectral capability would open up several possibilities for remote sensing. In assembling the sensor payloads we have primarily used off the shelf parts. This is an important consideration, because the detectors fly in hazardous conditions and could easily be lost or destroyed. The sensors need to be cheap and considered expendable, because if any particular sensor is thought to be too expensive to risk flying then it is unlikely ever to become a useful asset.

Acknowledgments

We gratefully acknowledge support of the Site-Directed Research and Development Program of Mission Support and Test Services LLC. We would like to thank Mark Adan, Howard Bender, Don Bintz, John Bird, Edward Bravo, Keith Chase, Dan Haber, Joann Jackson-Bass, Tom Keenan, Mike Madlener, Rusty Malchow, Karen McCall, Chris Melchor, Drew Morgan, Mark Norsworthy, Justin Sands, Bill Tremblay, and Hovig Yaralian for their contributions to this work.

References

BEE13: DOE/NV--711 Rev 3, available from
https://www.nsss.gov/docs/fact_sheets/DOENV_711.pdf

KAL60: Kalman, Rudolph Emil, “A New Approach to Linear Filtering and Prediction Problems”, *Transactions of the ASME-Journal of Basic Engineering* **82**, Series D, 35–45, 1960.

YAN10: Yang, Wei and Zurbenko, Igor, “Kolmogorov–Zurbenko filters”, *Wiley Interdisciplinary Reviews: Computational Statistics* **2** (3), 340–351 (2010), doi=10.1002/wics.71.

SAV64: Savitzky, A.; Golay, M.J.E. (1964). “Smoothing and Differentiation of Data by Simplified Least Squares Procedures”, *Analytical Chemistry* **36** (8): 1627–39 (1964), doi:10.1021/ac60214a047.

SMI97: Steven W. Smith, *The Scientist & Engineer's Guide to Digital Signal Processing, 1st Edition*, California Technical Publishing, Poway, California, **ISBN-13:** 978-0966017632 (1997).

NOTICE

This manuscript has been authored by Mission Support and Test Services, LLC, under Contract No. DE-NA0003624 with the U.S. Department of Energy and supported by the Site-Directed Research and Development Program, National Nuclear Security Administration, NA-22 USDOE Office of Defense Nuclear Nonproliferation

UNCLASSIFIED

UNCLASSIFIED

Research and Development (NA-22). The United States Government retains and the publisher, by accepting the article for publication, acknowledges that the United States Government retains a non-exclusive, paid-up, irrevocable, worldwide license to publish or reproduce the published form of this manuscript, or allow others to do so, for United States Government purposes. The U.S. Department of Energy will provide public access to these results of federally sponsored research in accordance with the DOE Public Access Plan (<http://energy.gov/downloads/doe-public-access-plan>). The views expressed in the article do not necessarily represent the views of the U.S. Department of Energy or the United States Government. DOE/NV/03624--0359.